

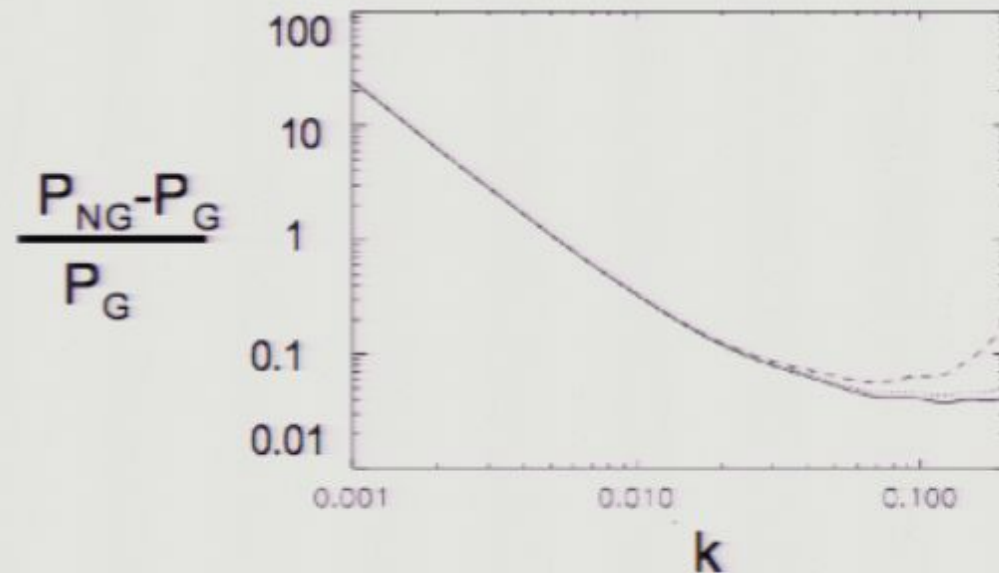
Title: The effect of primordial non gaussianity on large scale structure

Date: Mar 09, 2008 04:10 PM

URL: <http://pirsa.org/08030062>

Abstract:

## Non-Gaussianity with Large-scale structure



Licia Verde

ICREA & ICE (IEEC/CSIC) Barcelona

<http://www.ice.csic.es/personal/verde/>

Simplest inflationary models predict SMALL deviations from Gaussian initial conditions

How small is small? In some models “small” can be “detectable”

There can always be non-standard models (strings, defects etc. yielding primordial non-gaussianity)

# Inflationary predictions for $f_{\text{NL}}$

| Models  | $f_{\text{NL}}$  | Comments  |
|---|--|---|
| Single-field inflation  | $\mathcal{O}(\epsilon, \eta)$  | $\epsilon, \eta$ slow-roll parameters   |
| Curvaton scenario   | $\frac{5}{4r} - \frac{5}{6}r - \frac{5}{3}$  | $r \approx \left(\frac{\rho_{\text{curv}}}{\rho}\right)_{\text{decay}}$   |
| Inhomogeneous reheating   | $-\frac{5}{4} - I$   | $I = -\frac{5}{2} + \frac{5}{12} \frac{\Gamma}{\alpha \Gamma_1}$<br>“minimal case” $I = 0$ ( $\alpha = \frac{1}{6}$ , $\Gamma_1 = \bar{\Gamma}$ ) |
| Multiple scalar fields  | $\frac{p_s}{p_{\text{sc}}} \cos^2 \Delta \left(4 \cdot 10^3 \cdot \frac{V_{\text{xyx}}}{3H^2}\right) \cdot 60 \frac{H}{\chi}$    | order of magnitude estimate<br>of the absolute value  |
| Warm inflation  | $-\frac{5}{6} \left(\frac{\dot{\rho}_{\text{sc}}}{H^2}\right) \left[\ln\left(\frac{\Gamma}{H}\right) \frac{V'''}{\Gamma}\right]$ | $\Gamma$ : inflaton decay rate  |
| Ghost inflation   | $-85 \cdot \beta \cdot \alpha^{-8/5}$  | equilateral configuration   |
| DBI   | $-0.2 \gamma^2$  | equilateral configuration   |
| Preheating scenarios  | e.g. $\frac{M_{\text{pl}}}{\varphi_0} e^{Nq/2} \sim 50$  | $N$ : number of inflaton oscillations   |
| Inhomogeneous preheating and<br>inhomogeneous hybrid inflation                    | e.g. $\frac{5}{6} \lambda_{\varphi} \left(\frac{M_{\text{pl}}}{m_{\chi}}\right)^2 \sim 100$                                      | $\lambda_{\varphi}$ : inflaton coupling to the<br>waterfall field $\chi$  |
| Generalized single-field inflation<br>(including k-inflation and brane inflation) | $-\frac{35}{108} \left(\frac{1}{c_s^2} - 1\right) + \frac{5}{81} \left(\frac{1}{c_s^2} - 1 - 2\frac{\lambda}{\Sigma}\right)$     | high when the sound speed $c_s \ll 1$ or<br>$\lambda/\Sigma \gg 1$  |

Which means:

$f_{\text{NL}}$  Defined in Fourier space, through the bispectrum,  
and in general with complex dependence on  $k$  (vectors)

But many just say:  $\Phi = \phi + \alpha (\phi^2 - \langle \phi^2 \rangle)$

$f_{\text{NL}}$

Salopek Bond 1990; Gangui et al 1994;  
Verde et al 2000 (VWHK);  
Komatsu Spergel 2001

$f_{\text{NL}}$  Let's assume it is constant

Defined on Gravitational potential  
(actually Bardeen potential, important for sign)  
This evolves in a LCDM universe... more later

However other cases are possible:

VWHK

$$\Phi = \phi + \alpha(\phi^2 - \langle \phi^2 \rangle)$$

$$\delta = \phi + \alpha(\phi^2 - \langle \phi^2 \rangle) \quad \text{density}$$

Some two fields models (e.g. Luo Schramm 1994)

$$B \sim p^3$$

Some defect models

Different observables may be best suited for different types of non-gaussianity



# Searching for non-Gaussianity with LSS

clustering/spatial properties:

Bispectrum, trispectrum, etc.

warning: gravity also generates NG that's why  
trispectrum may be interesting (LV & Heavens 2001)

abundance of rare events:

by looking at the tails of the halo mass function

warning: what's a halo and what's its mass? What mass  
function?

anyway interesting: can probe smaller scales than CMB

## Why Trispectrum?

$$\begin{aligned} \langle \delta_{\mathbf{k}_1} \delta_{\mathbf{k}_2} \delta_{\mathbf{k}_3} \delta_{\mathbf{k}_4} \rangle &= \\ \langle \delta_{\mathbf{k}_1} \delta_{\mathbf{k}_2} \rangle \langle \delta_{\mathbf{k}_3} \delta_{\mathbf{k}_4} \rangle &+ (2 \text{ perms.}) + \langle \delta_{\mathbf{k}_1} \delta_{\mathbf{k}_2} \delta_{\mathbf{k}_3} \delta_{\mathbf{k}_4} \rangle_c \end{aligned}$$

where

$$\begin{aligned} \langle \delta_{\mathbf{k}_i} \delta_{\mathbf{k}_j} \rangle &= (2\pi)^3 P(k_i) \delta^D(\mathbf{k}_i + \mathbf{k}_j) \\ \langle \delta_{\mathbf{k}_1} \delta_{\mathbf{k}_2} \delta_{\mathbf{k}_3} \delta_{\mathbf{k}_4} \rangle_c &= (2\pi)^3 T(\mathbf{k}_i) \delta^D(\mathbf{k}_1 + \mathbf{k}_2 + \mathbf{k}_3 + \mathbf{k}_4). \end{aligned}$$

For mildly non-linear fields the 2OPT contribution to  $\langle \delta_{\mathbf{k}_1} \delta_{\mathbf{k}_2} \delta_{\mathbf{k}_3} \delta_{\mathbf{k}_4} \rangle$  is zero.

$$\begin{aligned} &\langle \delta_{\mathbf{k}_1} \delta_{\mathbf{k}_2} \delta_{\mathbf{k}_3} \delta_{\mathbf{k}_4} \rangle \\ &= (2\pi)^6 P(k_1) P(k_2) \delta^D(\mathbf{k}_1 + \mathbf{k}_3) \delta^D(\mathbf{k}_2 + \mathbf{k}_4) + cyc. \\ &+ \tau \sqrt{P(k_1) P(k_2) P(k_3) P(k_4)} \delta^D(\mathbf{k}_1 + \mathbf{k}_2 + \mathbf{k}_3 + \mathbf{k}_4), \end{aligned}$$

$$\tau \equiv \frac{T(\mathbf{k}_1, \mathbf{k}_2, \mathbf{k}_3, \mathbf{k}_4)}{\sqrt{P(k_1) P(k_2) P(k_3) P(k_4)}}$$



# Searching for non-Gaussianity with LSS

Clustering; inflation-type

Verde et al. (1999) and Scoccimarro et al. (2004) showed that constraints on primordial NG in the gravitational potential from large redshift-surveys like 2dF and SDSS are not competitive with CMB ones :  $f_{NL}$  has to be larger than  $10^2$ -  $10^3$  in order to be detected as a sort of non- linear bias in the galaxy-to-dark matter density relation. However LSS gives complementary constraints as it tests different scales than CMB.

Going to redshift  $z \sim 2$  can make LSS competitive (Sefusatti & Komatsu 2007). Going to higher  $z$  (e.g. through SZ cluster surveys or via 21-cm background anisotropies) helps, as the effective NG strength in the underlying CDM overdensity scales like  $(1+z)$  (Pillepich, Porciani & Matarrese 2006; Cooray 2006).

Why?

Back to VWHK

$$\Phi = \phi + \alpha(\phi^2 - \langle \phi^2 \rangle)$$

$$B(\mathbf{k}_1, \mathbf{k}_2, \mathbf{k}_3) \simeq \left\{ P(k_1)P(k_2) \left[ \left( 2\alpha \frac{\mathcal{M}_{k_3}}{\mathcal{M}_{k_1}\mathcal{M}_{k_2}} \right) + 2J(\mathbf{k}_1, \mathbf{k}_2) \right] \right\} + cyc.$$

$f_{NL}$  gravity

$$\delta(k, z) = \mathcal{M}_k(z)\Phi(k), \text{ where } \mathcal{M}_k(z) = \frac{2k^2 T(k)(1+z)}{3H_0^2}.$$

In '99 did  
not take  $\Lambda$   
seriously

!

In 1999 I did not think one could measure the galaxy bispectrum at  $z > 0$ ,  
and disentangle it from bias



# Searching for non-Gaussianity with LSS

## PDF

Primordial non-Gaussianity also strongly affects the abundance of the first non-linear objects in the Universe, thereby modifying the reionization history

It also affect the abundance of rare events such as massive clusters or high- $z$  galaxies and their formation redshift

Table 1. Minimum  $|\epsilon_A|$  and  $|\epsilon_B|$  detectable form different observables and their sign when positive skewness is required for detection. For Model A the primordial skewness has the same sign as  $\epsilon_A$ , while for Model B the primordial skewness has the opposite sign as  $\epsilon_B$ . In detecting non-zero  $\epsilon_{A,B}$  from CMB maps, the sign of the skewness does not influence the accuracy of the detection of non-Gaussianity, but, when using the abundance of high-redshift objects it is robust to detect non-Gaussianity that produces an excess rather than a defect in the number density. Only a positively skewed primordial distribution will generate more high-redshift objects than predicted in the Gaussian case.

| Observable     | Min. $ \epsilon_A $           | Min. $ \epsilon_B $ |
|----------------|-------------------------------|---------------------|
| CMB            | $10^{-3} \sim 10^{-2}$        | 20                  |
| LSS            | $10^{-2}$                     | $10^3 \sim 10^4$    |
| High- $z$ obj. | (+) $5 \times 10^{-4}$ (gal.) | (-) 200 (clusters)  |
| ST relation    | (+) $3 \times 10^{-3}$        | (-) 500             |

# Conventions:

- Sign: if  $\Phi_A = \Phi_{A,G} + \tilde{f}_{NL}(\Phi_{A,G}^2 - \langle \Phi_{A,G}^2 \rangle)$   
gravitational potential, then  $\tilde{f}_{NL} = -f_{NL}$

LSS crowd

Also:  $\zeta = \zeta_L - \frac{3}{5} f_{NL}^M \zeta_L^2$  Maldacena(2003)

- Amplitude:  $f_{NL}^{LSS} = g(\infty)/g(0) f_{NL}^{CMB}$

Warning: the same authors may use different conventions in different papers;  
Should we find an agreement?



# Searching for non-Gaussianity with rare events

- Besides using standard statistical estimators, like bispectrum, trispectrum, three and four-point function, skewness, etc. ..., one can look at the tails of the distribution, i.e. at rare events.
- Rare events have the advantage that they often maximize deviations from what predicted by a Gaussian distribution, but have the obvious disadvantage of being ... rare!
- Matarrese LV & Jimenez (2000) and Verde, Jimenez, Kamionkowski & Matarrese showed that clusters at high redshift ( $z > 1$ ) can probe NG down to  $f_{NL} \sim 10^2$  which is, however, not competitive with future CMB (Planck) constraints.
- For other type of non-gaussianity rare events may be competitive.

Improved formula obtained by LoVerde et al.



Matarrese, LV & Jimenez (2000):

Try to derive the mass function for non-gaussian fields

$$P(\psi) \equiv \langle \delta^D(\phi + \epsilon(\phi^2 - \langle \phi^2 \rangle) - \psi) \rangle \equiv \int d\phi P(\phi) \delta^D(\phi + \epsilon(\phi^2 - \langle \phi^2 \rangle) - \psi)$$

If no filtering

$$\delta_R(\mathbf{x}) = \phi_R(\mathbf{x}) + \epsilon \int d^3y F_R(|\mathbf{x} - \mathbf{y}|) \phi^2(\mathbf{y}) - C$$

With filtering

$$\begin{aligned} P(\delta_R) &= \langle \delta^D \left( \phi_R(\mathbf{x}) + \epsilon \int d^3y F_R(|\mathbf{x} - \mathbf{y}|) \phi^2(\mathbf{y}) - C - \delta_R(\mathbf{x}) \right) \rangle \\ &= \int [\mathcal{D}\phi] \mathcal{P}[\phi] \int \frac{d\lambda}{2\pi} \exp \left[ i\lambda \left( \phi_R(\mathbf{x}) + \epsilon \int d^3y F_R(|\mathbf{x} - \mathbf{y}|) \phi^2(\mathbf{y}) - C - \delta_R(\mathbf{x}) \right) \right] \end{aligned}$$

And that's when you learn to love path integrals

$$\mathcal{W}(\lambda) = -\frac{\lambda^2}{2}\mu_{2,R}^{(1)} - \epsilon\frac{i\lambda^3}{6}\mu_{3,R}^{(1)} \quad (\dots)$$

Cumulant generator

$$\mu_{2,R} \equiv \sigma_R^2 \equiv \langle \delta_R^2 \rangle \quad \mu_{3,R} \equiv \langle \delta_R^3 \rangle$$

In the Press-Schechter approach

$$P(> \delta_c | z_c, R) = \int_{\delta_c(z_c)}^{\infty} d\delta_R P(\delta_R) = \int_{\delta_c(z_c)}^{\infty} d\delta_R \int_{-\infty}^{\infty} \frac{d\lambda}{2\pi} e^{-i\lambda\delta_R + \mathcal{W}(\lambda)}$$

MVJ: exchange order of integration, integrate in  $\delta$

$$P(> \delta_c | z_c, R) = \frac{1}{2\pi i} \int_{-\infty}^{\infty} \frac{d\lambda}{\lambda} \exp[-i\lambda\delta_c(z_c) + \mathcal{W}(\lambda)] + \frac{1}{2} \quad \text{Exact so far..}$$

Truncate  $\mathcal{W}$  to first order in  $\epsilon$  and use saddle-point ( $\delta_c \gg 1$ ) to do the integral

$$P(> \delta_c | z_c, R) \approx \frac{1}{\sqrt{2\pi}} \frac{\sigma_R}{\delta_c(z_c)} \exp \left[ -\frac{1}{2} \frac{\delta_c^2(z_c)}{\sigma_R^2} \left( 1 - \frac{S_{3,R}}{3} \delta_c(z_c) \right) \right]$$

Resulting in:

$$P(> \delta_c | z_c, R) \approx \frac{1}{\sqrt{2\pi}} \frac{\sigma_R}{\delta_c(z_c)} \exp \left[ -\frac{1}{2} \frac{\delta_c^2(z_c)}{\sigma_R^2} \left( 1 - \frac{S_{3,R}}{3} \delta_c(z_c) \right) \right]$$

i.e. Gaussian mass function with  $\delta_c(z_c) \rightarrow \delta_c(z_c) \left[ 1 - \frac{S_{3,R}}{3} \delta_c(z_c) \right]^{1/2}$

**NB**

$$n(M, z_c) = f \frac{3H_0^2 \Omega_{0m}}{8\pi G M} \left| \frac{dP(> \delta_c | z_c, R)}{dM} \right|$$



## Is this competitive?

Note: this was derived in the Press-Schechter framework. PS fails at some point (spherical collapse etc.).

Recommended: use the ratio  $NG/G$  (compare this to observations normalized to numerically calibrated Gaussian predictions)

## TEST on simulations!

Approximations:

Linear terms in fNL

High-peaks saddle point

PS-type derivation

Pirsa: 08030062

**Table 1.** Minimum  $|\epsilon_A|$  and  $|\epsilon_B|$  detectable from different observables and their sign when positive skewness is required for detection. For Model A the primordial skewness has the same sign as  $\epsilon_A$ , while for Model B the primordial skewness has the opposite sign as  $\epsilon_B$ . In detecting non-zero  $\epsilon_{A,B}$  from CMB maps, the sign of the skewness does not influence the accuracy of the detection of non-Gaussianity, but, when using the abundance of high-redshift objects it is robust to detect non-Gaussianity that produces an excess rather than a defect in the number density. Only a positively skewed primordial distribution will generate more high-redshift objects than predicted in the Gaussian case.

| Observable     | Min. $ \epsilon_A $           | Min. $ \epsilon_B $ |
|----------------|-------------------------------|---------------------|
| CMB            | $10^{-3} \sim 10^{-2}$        | 20                  |
| LSS $z=0$      | $10^{-2}$                     | $10^3 \sim 10^4$    |
| High- $z$ obj. | (+) $5 \times 10^{-4}$ (gal.) | (-) 200 (clusters)  |
| ST relation    | (+) $3 \times 10^{-3}$        | (-) 500             |

## Is this competitive?

Note: this was derived in the Press-Schechter framework. PS fails at some point (spherical collapse etc.).

Recommended: use the ratio  $NG/G$  (compare this to observations normalized to numerically calibrated Gaussian predictions)

## TEST on simulations!

Approximations:

Linear terms in  $fNL$

High-peaks saddle point

PS-type derivation

Pirsa: 08030062

**Table 1.** Minimum  $|\epsilon_A|$  and  $|\epsilon_B|$  detectable from different observables and their sign when positive skewness is required for detection. For Model A the primordial skewness has the same sign as  $\epsilon_A$ , while for Model B the primordial skewness has the opposite sign as  $\epsilon_B$ . In detecting non-zero  $\epsilon_{A,B}$  from CMB maps, the sign of the skewness does not influence the accuracy of the detection of non-Gaussianity, but, when using the abundance of high-redshift objects it is robust to detect non-Gaussianity that produces an excess rather than a defect in the number density. Only a positively skewed primordial distribution will generate more high-redshift objects than predicted in the Gaussian case.

| Observable     | Min. $ \epsilon_A $           | Min. $ \epsilon_B $ |
|----------------|-------------------------------|---------------------|
| CMB            | $10^{-3} \sim 10^{-2}$        | 20                  |
| LSS $z=0$      | $10^{-2}$                     | $10^3 \sim 10^4$    |
| High- $z$ obj. | (+) $5 \times 10^{-4}$ (gal.) | (-) 200 (clusters)  |
| ST relation    | (+) $3 \times 10^{-3}$        | (-) 500             |

LV, Jimenez, Kamionkowski, Matarrese 2001



# N-body simulations of local (constant $f_{NL}$ ) NG

M. Grossi, K. Dolag, E. Branchini, S. Matarrese & L. Moscardini 2007

- | Standard CDM “concordance” model with:  $\Omega_{m0}=0.3$ ,  $\Omega_{\Lambda0}=0.7$ ,  $h=0.7$ ,  $\sigma_8=0.9$ ,  $n=1$
- | 9 models with:  $f_{NL} = -2000, -1000, -500, -100, 0, +100, +500, +1000, +2000$
- | **800<sup>3</sup> particles**, corresponding to a mass-resolution of  $m_p \approx 2 \cdot 10^{10}$  solar masses
- | Cosmological boxes:  **$L=500^3$  (Mpc/h)<sup>3</sup>**
- | Computations performed at **CINECA Supercomputing Centre** (Bologna) on a3k (only initial conditions) and sp5 machines: about 3000/5000 hours of CPU time per simulation. A second set of simulations has run at **MPA** (Garching).

see also recent related work by Dalal et al. 2007

## Is this competitive?

Note: this was derived in the Press-Schechter framework. PS fails at some point (spherical collapse etc.).

Recommended: use the ratio  $NG/G$  (compare this to observations normalized to numerically calibrated Gaussian predictions)

## TEST on simulations!

Approximations:

Linear terms in  $fNL$

High-peaks saddle point

PS-type derivation

Pirsa: 08030062

**Table 1.** Minimum  $|\epsilon_A|$  and  $|\epsilon_B|$  detectable from different observables and their sign when positive skewness is required for detection. For Model A the primordial skewness has the same sign as  $\epsilon_A$ , while for Model B the primordial skewness has the opposite sign as  $\epsilon_B$ . In detecting non-zero  $\epsilon_{A,B}$  from CMB maps, the sign of the skewness does not influence the accuracy of the detection of non-Gaussianity, but, when using the abundance of high-redshift objects it is robust to detect non-Gaussianity that produces an excess rather than a defect in the number density. Only a positively skewed primordial distribution will generate more high-redshift objects than predicted in the Gaussian case.

| Observable     | Min. $ \epsilon_A $           | Min. $ \epsilon_B $ |
|----------------|-------------------------------|---------------------|
| CMB            | $10^{-3} \sim 10^{-2}$        | 20                  |
| LSS $z=0$      | $10^{-2}$                     | $10^3 \sim 10^4$    |
| High- $z$ obj. | (+) $5 \times 10^{-4}$ (gal.) | (-) 200 (clusters)  |
| ST relation    | (+) $3 \times 10^{-3}$        | (-) 500             |

LV, Jimenez, Kamionkowski, Matarrese 2001

Page 20/41



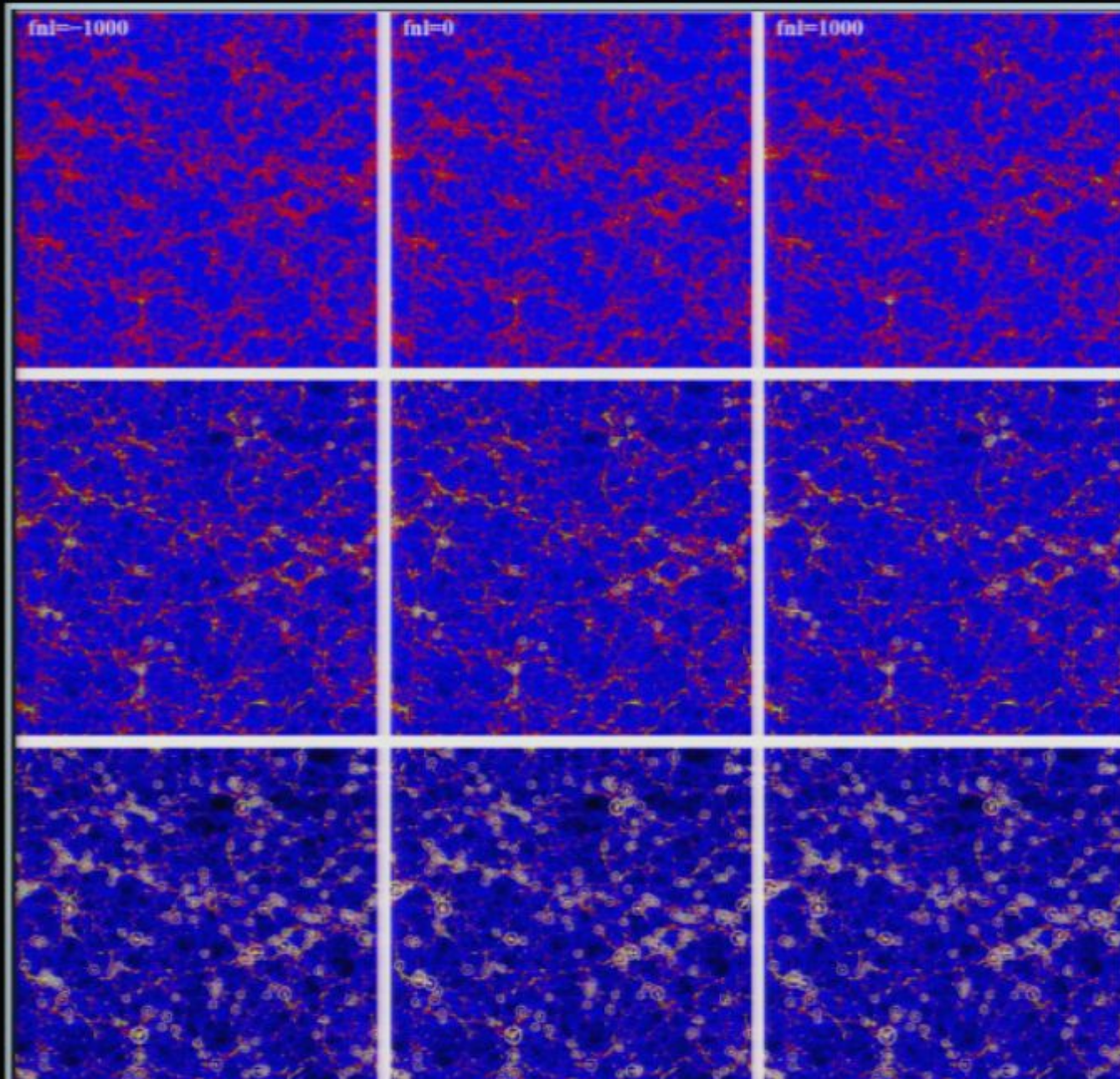
# N-body simulations of local (constant $f_{NL}$ ) NG

M. Grossi, K. Dolag, E. Branchini, S. Matarrese & L. Moscardini 2007

- | Standard CDM “concordance” model with:  $\Omega_{m0}=0.3$ ,  $\Omega_{\Lambda0}=0.7$ ,  $h=0.7$ ,  $\sigma_8=0.9$ ,  $n=1$
- | 9 models with:  $f_{NL} = -2000, -1000, -500, -100, 0, +100, +500, +1000, +2000$
- | **800<sup>3</sup> particles**, corresponding to a mass-resolution of  $m_p \approx 2 \cdot 10^{10}$  solar masses
- | Cosmological boxes:  **$L=500^3$  (Mpc/h)<sup>3</sup>**
- | Computations performed at **CINECA Supercomputing Centre** (Bologna) on a3k (only initial conditions) and sp5 machines: about 3000/5000 hours of CPU time per simulation. A second set of simulations has run at **MPA** (Garching).

see also recent related work by Dalal et al. 2007

# DM halos in NG simulations





# DM halo mass-function in NG models

M. Grossi, K. Dolag, E. Branchini, S. Matarrese & L. Moscardini 2007

Deviations from the Gaussian mass-function in excellent agreement with the theoretical predictions by Matarrese, Verde & Jimenez (2000):

$$F_{NG}(M, z, f_{NL}) \simeq \frac{1}{6} \frac{\delta_c^2(z_c)}{\delta_*(z_c)} \frac{dS_{3,M}}{d \ln \sigma_M} + \frac{\delta_*(z_c)}{\delta_c(z_c)}$$

where  $F_{NG}$  represents the NG/G mass-function ratio

$$n(M, z, f_{NL}) = n_G(M, z) F_{NG}(M, z, f_{NL})$$

and

$$\delta_*(z_c) = \delta_c(z_c) \sqrt{1 - S_{3,M} \delta_c(z_c)/3},$$

with  $S_{3,M}$  the skewness of the mass-density field on scale M

$$S_{3,M} \equiv \frac{\langle \delta_M^3 \rangle}{\sigma_M^3} \propto -f_{NL}$$

Pirsa: 08030062

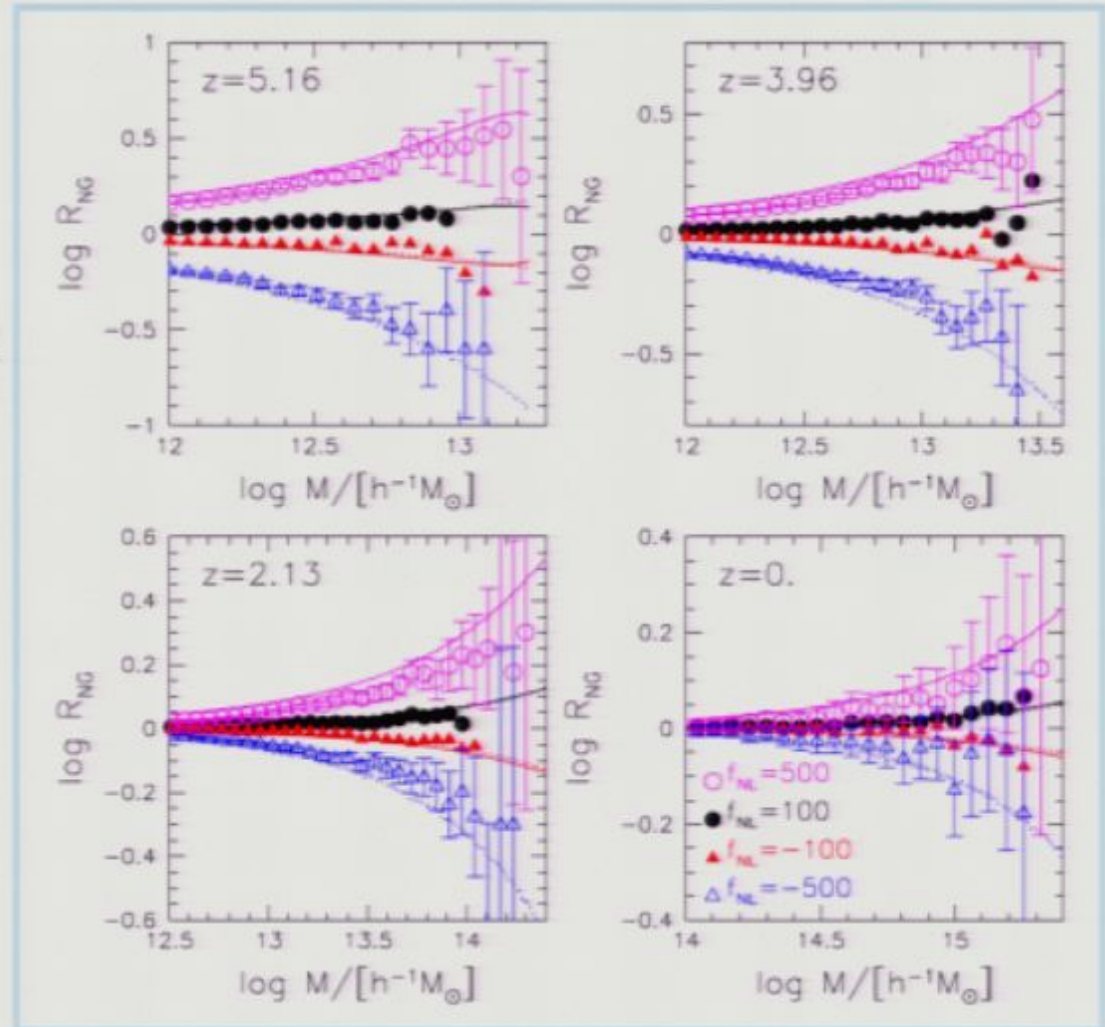
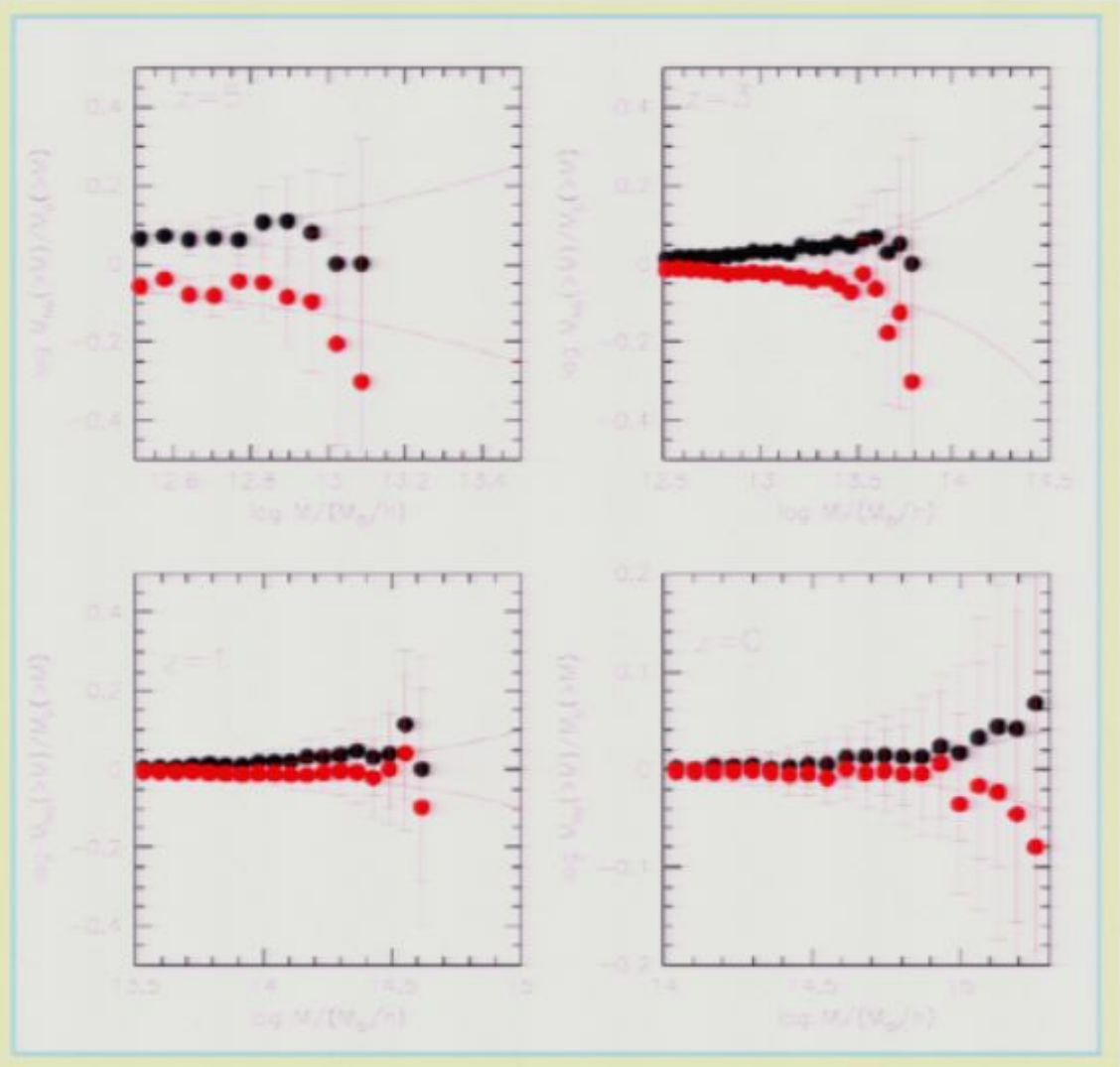


Figure 3. Logarithm of the ratio of the halo cumulative mass functions  $R_{NG}$  as a function of the mass is shown in the different panels at the same redshifts as in Fig. 1. Circles and triangles refer to positive and negative values for  $f_{NL}$ ; open and filled symbols refer to  $f_{NL} = \pm 500$  and  $f_{NL} = \pm 100$ , respectively. Theoretical predictions obtained starting from eqs (3) and (4) are shown by dotted and solid lines, respectively. Poisson errors are shown for clarity only for the cases  $f_{NL} = \pm 500$ .



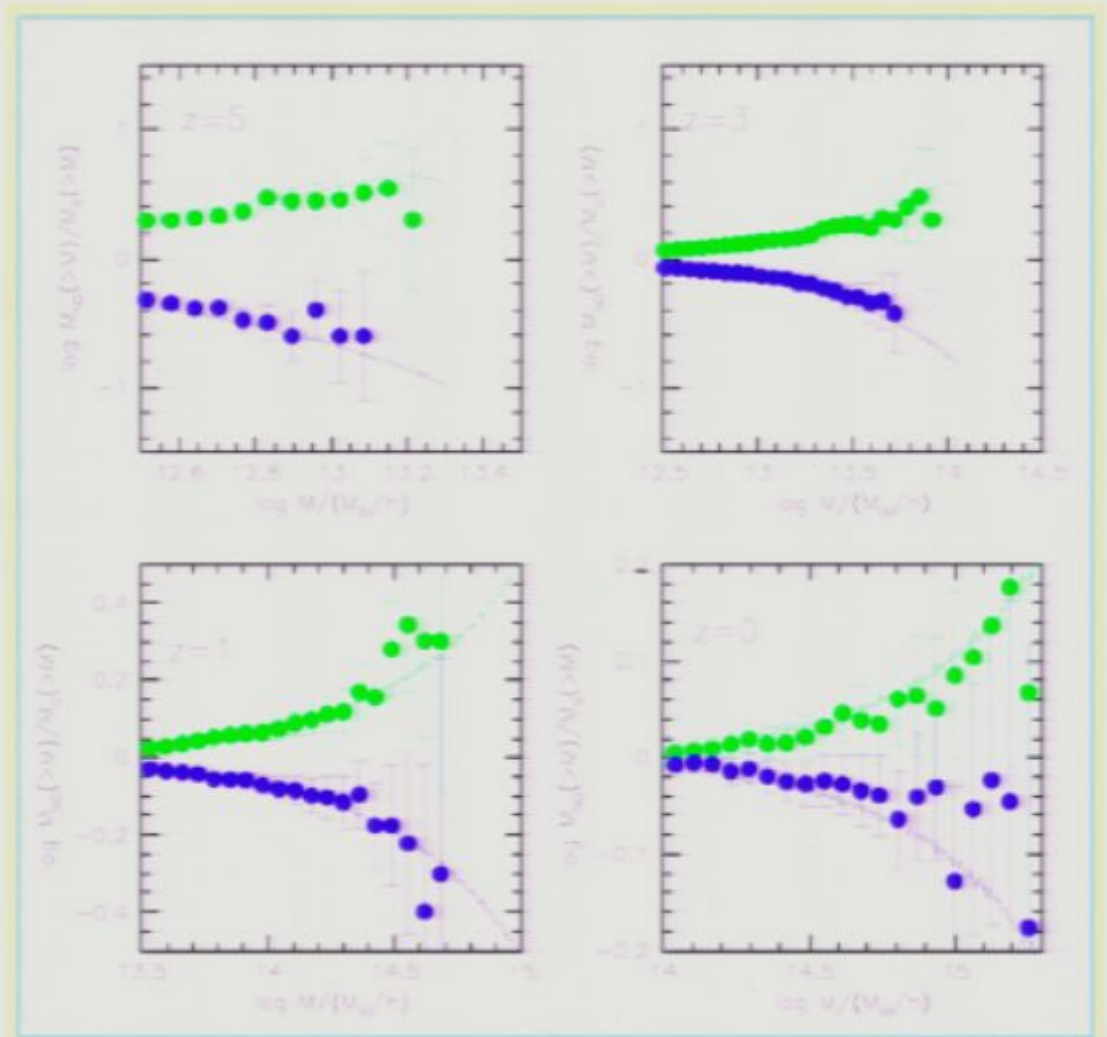
$$f_{\text{NL}} = \pm 100$$

Continuous line: ratio of Press-Schechter-like formula from Matarrese, Verde & Jimenez, 2000 to Gaussian mass-function



$$f_{\text{NL}} = \pm 500$$

The agreement with the MVJ formula is encouraging because it allows to make predictions for a large class of models without running many expensive N-body simulations.



## LoVerde, Miller, Shandera LV 2007(8)

Among other things (see Marilena's talk)

$$P(> \delta_c | z_c, R) = \int_{\delta_c(z_c)}^{\infty} d\delta_R P(\delta_R) = \int_{\delta_c(z_c)}^{\infty} d\delta_R \int_{-\infty}^{\infty} \frac{d\lambda}{2\pi} e^{-i\lambda\delta_R + \mathcal{W}(\lambda)}$$

Remember this?

$$P(\delta_R) d\delta_R = \frac{d\delta_R}{2\pi i} \frac{1}{\sigma_R^2} \int_{-i\infty}^{i\infty} dy \exp \left[ \frac{y\delta_R}{\sigma_R^2} - \frac{S(y)}{\sigma_R^2} \right]$$

it is now written as

Saddle point  $\rightarrow$  Edgeworth expansion

$$P(\nu) d\nu = \frac{d\nu}{\sqrt{2\pi}} e^{-\nu^2/2} \left[ 1 + \sigma_R \frac{S_3(R)}{6} H_3(\nu) + \sigma_R^2 \left( \frac{S_4(R)}{24} H_4(\nu) + \frac{S_3(R)^2}{72} H_6(\nu) \right) + \dots \right]$$

where  $\nu = \delta_R / \sigma_R$  and the  $H_n$  are Hermite polynomials

$$\mathbf{v} = \delta / \sigma$$

$$H_3(\nu) = \nu^3 - 3\nu$$

$$H_4(\nu) = \nu^4 - 6\nu^2 + 3$$

$$H_6(\nu) = \nu^6 - 15\nu^4 + 45\nu^2 - 15.$$

To finally give:

$$P(> \delta_c | z_c, M) = \frac{1}{2} \left[ 1 - \operatorname{erf} \left( \frac{\delta_c}{\sqrt{2}\sigma_M} \right) \right] - \frac{S_3(M)\sigma_M}{3!} \left( 1 - \left( \frac{\delta_c}{\sigma_M} \right)^2 \right) \frac{e^{-\frac{\delta_c^2}{2\sigma_M^2}}}{\sqrt{2\pi}} + \dots$$

Different approximations: High peaks ---> MVJ  
lower peaks--->LVSMV

Must be tested on simulations, of course.

How different?

For small NG and high peaks the ratio NG/G  $P(>\delta)$

$$1 + S_3 \delta_c^3 / (6 \sigma_R^2)$$

For both expressions



So is there agreement or disagreement with simulations?

Resolution issues, simulation issues, initial conditions etc.....

Compare simulations  
&  
Initial conditions!!!



# DM halo bias as a constraint on NG

Interesting paper: arXiv:0710.4560

The imprints of primordial non-gaussianities on large-scale structure: scale dependent bias and abundance of virialized objects

Neal Dalal,<sup>1</sup> Olivier Doré,<sup>1</sup> Dragan Huterer,<sup>2,3</sup> and Alexander Shirokov<sup>1</sup>

<sup>1</sup> *Canadian Institute for Theoretical Astrophysics, 60 St. George St,  
University of Toronto, Toronto, ON, Canada M5S3H8*

<sup>2</sup> *Kavli Institute for Cosmological Physics and Department of  
Astronomy and Astrophysics, University of Chicago, Chicago, IL 60637*

<sup>3</sup> *Department of Physics, University of Michigan, 450 Church St, Ann Arbor, MI 48109*

(Received February 2, 2008)

We study the effect of primordial nongaussianity on large-scale structure, focusing upon the most massive virialized objects. Using analytic arguments and N-body simulations, we calculate the mass function and clustering of dark matter halos across a range of redshifts and levels of nongaussianity. We propose a simple fitting function for the mass function valid across the entire range of our simulations. We find pronounced effects of nongaussianity on the clustering of dark matter halos, leading to strongly scale-dependent bias. This suggests that the large-scale clustering of rare objects may provide a sensitive probe of primordial nongaussianity. We very roughly estimate that upcoming surveys can constrain nongaussianity at the level  $|f_{\text{NL}}| \lesssim 10$ , competitive with forecasted constraints from the microwave background.

# DM halo bias as a constraint on NG

Dalal, Dore', Huterer & Shirokov 2007

Dalal et al. (2007) have recently shown that the halo bias is sensitive to primordial non-Gaussianity through a scale-dependent correction term

$$\Delta b(k)/b \propto 2 f_{\text{NL}} \delta_c f(k)$$

This opens interesting prospects for constraining or measuring NG in LSS but demands for an accurate evaluation of the effects of (general) NG on halo biasing.

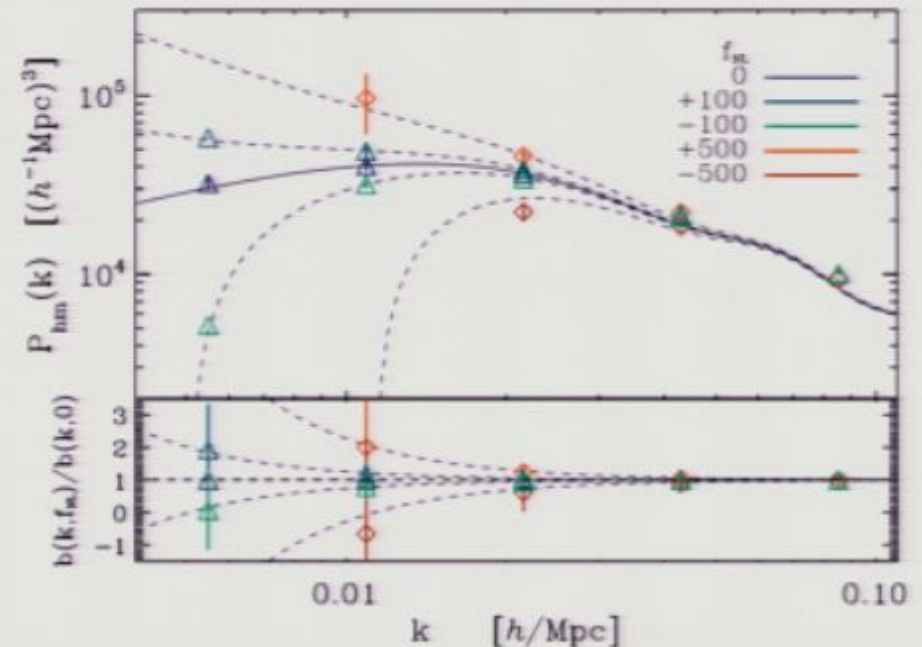


FIG. 7: Cross-power spectra for various  $f_{\text{NL}}$ . The upper panel displays  $P_{\text{hs}}(k)$ , measured in our simulations at  $z = 1$  for halos of mass  $1.6 \times 10^{13} M_{\odot} < M < 3.2 \times 10^{13} M_{\odot}$ . The solid line corresponds to the theoretical prediction for  $P_{\text{hs}}$  with a fitted bias  $b_0 = 3.25$ . We see a strongly scale-dependent correction to the bias for  $f_{\text{NL}} \neq 0$ , increasing towards small  $k$  (large scales). The bottom panel displays the ratio  $b(k, f_{\text{NL}})/b(k, f_{\text{NL}} = 0)$ . The errors are computed from the scatter amongst our simulations and within the bins. Triangles correspond to our large ( $1024^3$  particle) simulations whereas diamonds correspond to our smaller ( $512^3$  particle) simulations. The dotted lines correspond to our fit for the bias dependence on  $f_{\text{NL}}$  defined in Eq. (16).



# Clustering of peaks (DM halos) of NG density field

Start from results obtained in the 80's by

Grinstein & Wise 1986, ApJ, 310, 19

Matarrese, Lucchin & Bonometto 1986, ApJ, 310, L21

giving the general expression for the peak 2-point function as a function of N-point connected correlation functions of the background linear (i.e. Lagrangian) mass-density field

$$\xi_{h,M}(|\mathbf{x}_1 - \mathbf{x}_2|) = -1 +$$

$$\exp \left\{ \sum_{N=2}^{\infty} \sum_{j=1}^{N-1} \frac{\nu^N \sigma_R^{-N}}{j!(N-j)!} \xi^{(N)} \left[ \begin{matrix} \mathbf{x}_1, \dots, \mathbf{x}_1, & \mathbf{x}_2, \dots, \mathbf{x}_2 \\ j \text{ times} & (N-j) \text{ times} \end{matrix} \right] \right\}$$

(requires use of path-integral, cluster expansion, multinomial theorem and asymptotic expansion).

The analysis of NG models was motivated by a paper by Vittorio, Juszkiewicz and Davis (1986) on bulk flows.

THE ASTROPHYSICAL JOURNAL, 310:21-32, 1986 November 1.  
© 1986 The American Astronomical Society. All rights reserved. Printed in U.S.A.

## A PATH-INTEGRAL APPROACH TO LARGE-SCALE MATTER DISTRIBUTION ORIGINATED BY NON-GAUSSIAN FLUCTUATIONS

SARINO MATARRESE  
International School for Advanced Studies, Trieste, Italy

FRANCESCO LUCCHIN  
Dipartimento di Fisica G. Galilei, Padova, Italy

AND

SILVIO A. BONOMETTO  
International School for Advanced Studies, Trieste, Italy; Dipartimento di Fisica G. Galilei, Padova, Italy;  
and INFN, Sezione di Padova

Received 1986 July 2; accepted 1986 August 1

### ABSTRACT

The possibility that, in the framework of a biased theory of galaxy clustering, the underlying matter distribution be non-Gaussian itself, because of the very mechanisms generating its present status, is explored. We show that a number of contradictory results, seemingly present in large-scale data, in principle can recover full coherence, once the requirement that the underlying matter distribution be Gaussian is dropped. For example, in the present framework the requirement that the two-point correlation functions vanish at the same scale (for different kinds of objects) is overcome. A general formula, showing the effects of a non-Gaussian background on the expression of three-point correlations in terms of two-point correlations, is given.

Subject heading: galaxies: clustering

THE ASTROPHYSICAL JOURNAL, 310:19-22, 1986 November 1.  
© 1986 The American Astronomical Society. All rights reserved. Printed in U.S.A.

## NON-GAUSSIAN FLUCTUATIONS AND THE CORRELATIONS OF GALAXIES OR RICH CLUSTERS OF GALAXIES<sup>1</sup>

BENJAMIN GRINSTEIN<sup>2</sup> AND MARK B. WISE<sup>2</sup>  
California Institute of Technology

Received 1986 March 6; accepted 1986 April 28

### ABSTRACT

Natural primordial mass density fluctuations are those for which the probability distribution, for mass density fluctuations averaged over the horizon volume, is independent of time. This criterion determines that the two-point correlation of mass density fluctuations has a Zeldovich power spectrum (i.e., a power spectrum proportional to  $k$  at small wavenumbers) but allows for many types of reduced (connected) higher correlations. Assuming galaxies or rich clusters of galaxies arise wherever suitably averaged natural mass density fluctuations are unusually large, we show that the two-point correlation of galaxies or rich clusters of galaxies can have significantly more power at small wavenumbers (e.g., a power spectrum proportional to  $1/k$  at small wavenumbers) than the Zeldovich spectrum. This behavior is caused by the non-Gaussian part of the probability distribution for the primordial mass density fluctuations.

Subject headings: cosmology — galaxies: clustering



# Halo bias in NG models

- Matarrese & Verde 2008 (arXiv:0801.4826, ApJL in press) have applied this relation to the case of local NG (fNL-type), obtaining the power-spectrum of dark matter halos modeled as high “peaks” (upcrossing regions) of height  $v = \delta_c / \sigma_R$  of the underlying mass density field (Kaiser’s model). Here  $\delta_c(z)$  is the critical overdensity for collapse (at redshift  $z$ ) and  $\sigma_R$  is the *rms* mass fluctuation on scale  $R$  ( $M \sim R^3$ )
- Next, account for motion of peaks (going from Lagrangian to Eulerian space), which implies (Catelan et al. 1998)

$$1 + \delta_h(\mathbf{x}) = (1 + \delta_h(\mathbf{x}_L))(1 + \delta_R(\mathbf{x}))$$

and (to linear order)  $b = 1 + b_L$  (Mo & White 1996) to get the scale-dependent halo bias in the presence of NG initial conditions.

# Halo bias in NG models

$$P_{\text{halo}}(k, z) = \frac{\delta_c^2(z)}{\sigma_R^4 D^2(z)} P_{\delta\delta}(k, z) \left[ 1 + 4f_{\text{NL}} \delta_c(z) \frac{\mathcal{F}_R(k)}{\mathcal{M}_R(k)} \right]$$

$$b_{\text{h}}^{\text{fNL}} = 1 + \frac{\Delta_c(z)}{\sigma_R^2 D^2(z)} \left[ 1 + 2f_{\text{NL}} \frac{\Delta_c(z)}{D(z)} \frac{\mathcal{F}_R(k)}{\mathcal{M}_R(k)} \right]$$

form factor:

$$\mathcal{F}_R(k) = \frac{1}{8\pi^2 \sigma_R^2} \int dk_1 k_1^2 \mathcal{M}_R(k_1) P_{\phi}(k_1) \times \int_{-1}^1 d\mu \mathcal{M}_R(\sqrt{\alpha}) \left[ \frac{P_{\phi}(\sqrt{\alpha})}{P_{\phi}(k)} + 2 \right]$$

$$\alpha = k_1^2 + k^2 - 2k_1 k \mu$$

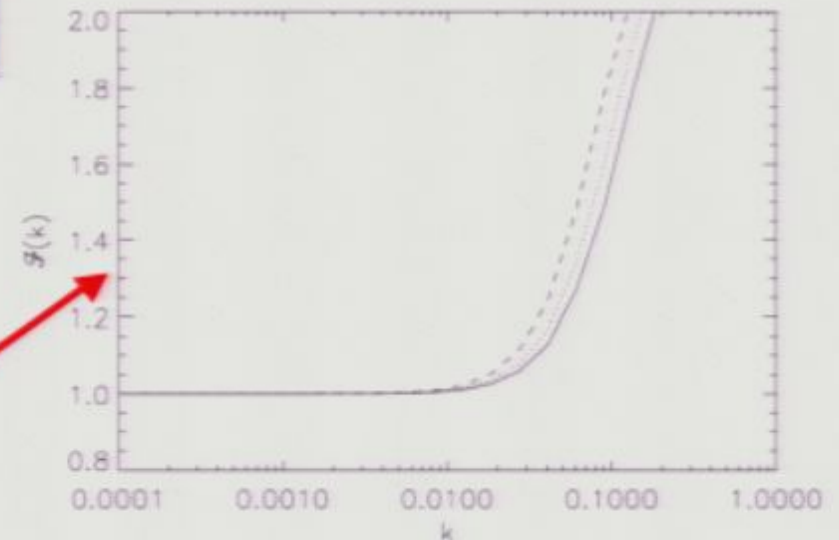


FIG. 1.— The function  $\mathcal{F}_R(k)$  for three different masses:  $1 \times 10^{14} M_{\odot}$  (solid),  $2 \times 10^{14} M_{\odot}$  (dotted),  $1 \times 10^{15} M_{\odot}$  (dashed).

factor connecting the smoothed linear overdensity with the primordial potential:

$$\mathcal{M}_R(k) = \frac{2}{3} \frac{T(k) k^2}{H_0^2 \Omega_{m,0}} W_R(k)$$

power-spectrum of a Gaussian gravitational potential

window function defining the radius  $R$  of a proto-halo of mass  $M(R)$ :

transfer function:

# Halo bias in NG models

$$\Delta P/P = 4f_{\text{NL}}\delta_c(z) \frac{\mathcal{F}_R(k)}{\mathcal{M}_R(k)}$$

- The NG correction to the halo bias is scale, mass and redshift dependent
- Neglecting the effect of the form factor  $\mathcal{F}_R(k)$ , of the transfer function  $T(k)$  and of the window function  $W_R(k)$  leads to an error of up to 100% in the NG bias correction and hence in  $f_{\text{NL}}$
- Large high-resolution N-body simulations should be used to accurately evaluate the effect (Grossi et al. in preparation)

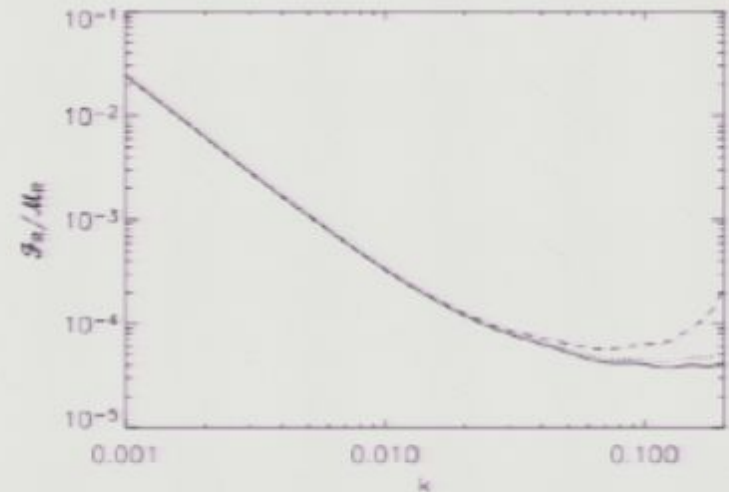


FIG. 3.— The scale dependence of  $\Delta b_h/b_h$  for three different masses:  $1 \times 10^{14} M_\odot$  (solid),  $2 \times 10^{14} M_\odot$  (dotted),  $1 \times 10^{15} M_\odot$  (dashed).

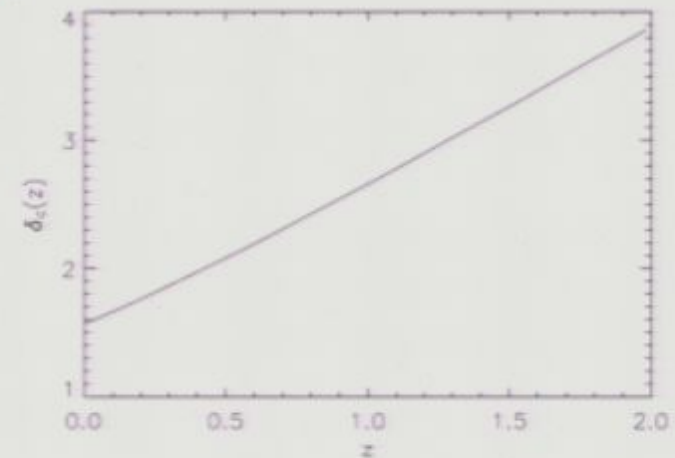


FIG. 2.— The redshift dependence of  $\Delta b_h/b_h$ .



# Halo bias in NG models

- Extension to general (scale and configuration dependent) NG is straightforward
- In full generality write the  $\phi$  bispectrum as  $B_\phi(k_1, k_2, k_3)$ . The relative NG correction to the halo bias is

$$\frac{\Delta b_h}{b_h} = \frac{\Delta_c(z)}{D(z)} \frac{1}{8\pi^2 \sigma_R^2} \int dk_1 k_1^2 \mathcal{M}_R(k_1) \times$$

$$\int_{-1}^1 d\mu \mathcal{M}_R(\sqrt{\alpha}) \frac{B_\phi(k_1, \sqrt{\alpha}, k)}{P_\phi(k)}$$

$$\alpha = k_1^2 + k^2 + 2k_1 k \mu$$

- It applies e.g. to non-local NG (DBI, etc.. )

# Halo bias in NG models

- Extension to general (scale and configuration dependent) NG is straightforward
- In full generality write the  $\phi$  bispectrum as  $B_\phi(k_1, k_2, k_3)$ . The relative NG correction to the halo bias is

$$\frac{\Delta b_h}{b_h} = \frac{\Delta_c(z)}{D(z)} \frac{1}{8\pi^2 \sigma_R^2} \int dk_1 k_1^2 \mathcal{M}_R(k_1) \times$$
$$\int_{-1}^1 d\mu \mathcal{M}_R(\sqrt{\alpha}) \frac{B_\phi(k_1, \sqrt{\alpha}, k)}{P_\phi(k)}$$
$$\alpha = k_1^2 + k^2 + 2k_1 k \mu$$

- It applies e.g. to non-local NG (DBI, etc.. )

# Conclusions & future prospects



# Conclusions & future prospects

- \* Constraining/detecting non-Gaussianity is a powerful tool to discriminate among competing scenarios for perturbation generation (*standard inflation, curvaton, modulated-reheating, DBI, ghost inflation, multi-field, etc. ...*) some of which imply large non-Gaussianity. Non-Gaussianity will soon become the smoking-gun for (non?)-standard inflation models.
- \* Constraining non-Gaussianity in LSS allows to put independent limits on NG and on a different range of scales. Massive/high redshift objects (rare events) are most sensitive to primordial non-Gaussianity, both in their abundance and clustering (bias).
- \* Predicting/constraining non-Gaussianity has become a branch of *Precision Cosmology* this requires accurate analytical calculations, high-resolution numerical simulations.

# PAU

<http://www.ice.csic.es/research/PAU/PAU-welcome.html>

Close collaboration between particle physicists (theorists and experimentalists) and astrophysicists (theorists and observers)

Awarded consolider-ingenio 2010

“Hybrid” technique: narrow band photometry New camera ( $\sim 3500\text{-}9000$  AA)

Survey  $\sim 10000$  deg<sup>2</sup>  $0.1 < z < 1.0$ ,  $\sim 14\text{M}$  LRG galaxies

Measures both  $H(z)$  and  $\text{Da}$  But just imagine what you can do with  $30\text{Gpc}^3$ , and  $\sim 200$  M galaxies

Instituto de fisica de alta energias (IFAE-Barcelona)

Instituto de ciencias del Espacio (ICE-Barcelona)

Instituto astrofisico de Andalucia (IAA-Granada)

Instituto de fisica teorica (IFT-Madrid)

Centro de investigaciones[...] (CIEMAT-Madrid)

Instituto de fisica corpuscolar (IFIC -Valencia)

Puerto de informacion Cientifica(PIC-Barcelona)



# Florence, Planck and LHC



The Galileo Galilei Institute for Theoretical Physics  
Arcetri, Florence



## January-March 2009 winter workshop New horizons for modern cosmology

Cosmology is offering us a new laboratory where standard and exotic fundamental theories can be tested on scales not otherwise accessible. The success of the standard cosmological model has many puzzling consequences and raises several key questions which are far from being answered. For example, the observation of dark energy demonstrates that our well established theories of particles and gravity are incomplete if not incorrect. What makes up the dark side of the universe? What created the primordial fluctuations? Is gravity purely geometry as envisaged by Einstein, or is there more to it (such as scalar partners and extra dimensions)?

An unprecedented experimental effort is currently being put into addressing these grand-challenges questions in cosmology. This is an intrinsically inter-disciplinary issue, and the range of opportunities afforded by the wealth of high precision data that will become available means that it will inevitably be at the forefront of research in astrophysics and fundamental physics in the coming decades. We aim to bring together scientists at the forefront of the field both on the experimental side and the theoretical side to discuss these issues.



No Signal

VGA-1